

Research Article

Reinforcement of Natural Rubber with Bacterial Cellulose via a Latex Aqueous Microdispersion Process

Sirilak Phomrak and Muenduen Phisalaphong

Chemical Engineering Research Unit for Value Adding of Bioresources, Department of Chemical Engineering, Faculty of Engineering, Chulalongkorn University, Bangkok 10330, Thailand

Correspondence should be addressed to Muenduen Phisalaphong; muenduen.p@chula.ac.th

Received 4 October 2016; Revised 26 November 2016; Accepted 4 January 2017; Published 9 February 2017

Academic Editor: Domenico Acierno

Copyright © 2017 Sirilak Phomrak and Muenduen Phisalaphong. This is an open access article distributed under the Creative Commons Attribution License, which permits unrestricted use, distribution, and reproduction in any medium, provided the original work is properly cited.

Natural rubber (NR) composites were reinforced with bacterial cellulose (BC) to improve mechanical and physical properties. The natural rubber bacterial cellulose (NRBC) composite films were prepared via a latex aqueous microdispersion process by a thorough mixing of BC slurry with natural rubber latex (NRL). The structural morphology and chemical and physical properties of NRBC composites were investigated. The hydrophilicity, opacity, and crystallinity of the NRBC composites were significantly enhanced because of the added BC. By loading BC at 80 wt.%, the mechanical properties, such as Young's modulus and tensile strength, were 4,128.4 MPa and 75.1 MPa, respectively, which were approximately 2,580 times and 94 times those of pure NR films, respectively, whereas the elongation at break of was decreased to 0.04 of that of the NR film. Because of its high mechanical strength and thermal stability, the NRBC composites have potential uses as high mechanical strength rubber-based products and bioelastic packaging in many applications.

1. Introduction

NRL is a milky fluid produced from rubber trees. NRL deteriorates when exposed to sunlight, ozone, and oxygen and can be coagulated by acidic reagents. NR is a polymer of isoprene (cis-1,4-polyisoprene) made from NRL [1]. Thailand is the world's largest NR exporter, and about 85–90% of Thailand NR products have been exported to China, Malaysia, Europe, Japan, Republic of Korea, and the United States (according to the reports from The Thai Rubber Association in 2001–2015). To add more value and expand commercial utilization of NR, research and development of NR-based products are required.

NR has the ability to regain its original shape after being deformed. Because of the outstanding elastic properties of NR, it has been used as a major raw material in the elastomer industry, including applications as automobile and truck tires, gloves, food wrap, and plastic bags or flexible packaging. However, some properties of NR, such as low mechanical strength and low abrasion resistance, limit product applications. Moreover, its mechanical properties

vary with temperature. The softness of NR increases with increasing temperature, whereas brittleness increases at low temperatures. Thus, structural modification is required to improve NR properties [1, 2]. Reinforcement is a simple method to reduce defects. The reinforcement of NR depends on reinforcing agents such as fibers and nanoparticles [3]. Nanoscale additives, such as carbon black and silica nanoparticles, have been commonly used as polymer reinforcing agents [4, 5]. Silica-reinforced NR prepared via a sol-gel process is promising and has been widely used [6, 7]. The modification of NR by grafting with high polar polymer such as poly(methyl methacrylate) or PMMA to improve the compatibility between NR and silica particles was prepared for enhanced performance of NR reinforcement [7–9]. Research studies for reinforcing additives have included glass fiber, aramid, nylon, graphene, sago starch, clay, attapulgite, carbon nanotubes and lignocellulosic fiber, wood flour, oil palm flour, cotton fiber, and microcrystalline cellulose [10, 11]. Regarding green material development, NR and cellulose are major biopolymers and renewable materials of high availability in Southeast Asia. Additionally, nanocellulose

produced by the bacteria *Acetobacter xylinum*, called bacterial cellulose (BC), has been studied for the use in both natural and synthetic polymer reinforcing [12–16]. However, low concentrations of nonpretreated plant cellulose fibers and BC nanofibers [17] could be added to the NR matrix because of the difference of polarities between NR and cellulose fibers. The development of NR-cellulose composite is limited by nonhomogeneous dispersion of cellulose particle in a rubber matrix. The preparation of NR composites via a latex aqueous microdispersion process instead of NR melt blending may help reduce the difference of polarities and increase the adhesion of cellulose fibers to the rubber matrix [17]. In addition, the size of nanofillers has significant effect on the strengths of composites; the increase of mechanical strength of NR composites with the decrease in size of reinforcing agent due to the homogeneous distribution was reported [18]. In this study, composite films of NR reinforced with BC nanofibers were developed via a latex aqueous microdispersion process. By means of adding BC in form of dilute slurry into NRL, much higher weight ratio of BC could be loaded into NRL with good BC fiber dispersion and distribution in NR matrix. After the composite films were fabricated, physical and chemical properties of the films were characterized for further applications.

2. Materials and Methods

2.1. Materials. NRL with 60 wt.% dry rubber content was purchased from the Rubber Research Institute of Thailand (Bangkok, Thailand). BC ($\approx 99\%$ water content in wet weight) was kindly provided by Pramote Thamarat from the Institute of Research and Development of Food Product, Kasetsart University (Bangkok, Thailand). All other chemical reagents were purchased from Sigma-Aldrich (Thailand) Co., Ltd. (Bangkok, Thailand).

2.2. BC Slurry Preparation. Small cubes of BC hydrogel ($1 \times 1 \times 1$ cm) were purified by washing with deionized (DI) water, soaked with 1 wt.% NaOH for 48 hours to remove bacterial cells, and were rinsed with DI water until the pH was 7.0. To prepare the BC slurry, BC was thoroughly crushed and homogenized using a blender at room temperature.

2.3. Characterization of the BC Slurry. Scanning electron microscopy (SEM) micrographs were taken on a JSM-5410LV (JEOL, Tokyo, Japan). BC slurry was dried and sputtered with a 200-Å layer of gold in a Balzers-SCD 040 sputter coater (Liechtenstein). The images were immediately viewed at a magnification of 20,000x and an accelerating voltage of 2 kV.

2.4. Preparation of NR Film and NRBC Composite Films. For the preparation of NR film, the NRL has to be diluted into 30 wt.% dry rubber content before fabrication. For the preparation of NRBC films, the dilute slurry of BC in DI water with BC of 1 g of dry weight/100 mL was added to NRL, and the mixture was thoroughly mixed using a mechanical stirrer for 5 minutes at room temperature. The mixtures were prepared for compositions by weight ratios of BC/NR at 20/80 (NRBC20), 50/50 (NRBC50), and 80/20 (NRBC80).

The weight ratios are expressed as wt.% on a dry basis. The films were fabricated by pouring prepared suspension into a tray, setting at room temperature for 3 hours and drying in an air convection oven at 50°C for 2 days.

2.5. Characterization of the Composite Films. Attenuated total reflectance Fourier transform infrared spectroscopy (ATR-FTIR) spectra of the films were measured at wavenumbers ranging $4000\text{--}600\text{ cm}^{-1}$ at a resolution of 4 cm^{-1} with a Nicolet SX-170 FTIR spectrometer (Thermo Scientific, Waltham, MA, USA).

Morphology of BC fibers and morphological structures of the films were examined by scanning electron microscope (SEM). The BC slurry and films were frozen in liquid nitrogen, vacuum-dried, and sputtered with gold prior to photograph. The images were immediately viewed at an accelerating voltage of 15 kV under SEM using a JOEL JSM-5410LV microscope (Tokyo, Japan).

The opacity of representative NR, BC, and NRBC composite films was measured using a UV-Vis Spectrophotometer (UV-2450, Shimadzu, Japan). Light transmission barrier properties were determined by measuring their light absorption at 600 nm (A_{600}). The degrees of opacity were the average values determined from three samples. The opacity was calculated as follows [19, 20]:

$$\text{Opacity} = \frac{A_{600}}{\text{Thickness (mm)}}. \quad (1)$$

The dynamic advancing and receding water contact angles under air at room temperature were measured using a contact angle goniometer (Ramé-hart, Instrument Co., Succasunna, NJ, USA, model 100-00), equipped with a Gilmont syringe and a 24-gauge flat-tipped needle.

The definitive structural information, crystallinity, interatomic distances, and bond angles were characterized by an X-ray diffractometer (model D8 Discover, Bruker AXS, Karlsruhe, Germany). X-ray diffraction patterns were recorded with CuK α radiation ($k = 1.54\text{ \AA}$). The operating voltage and current were 40 kV and 40 mA, respectively. Samples were scanned from $10\text{--}40^\circ 2\theta$ at a scan speed of 3° min^{-1} . Profile fitting and crystallinity (%) calculations were performed with Topas version 3.0 (Bruker, AXS) software.

Thermogravimetric analysis (TGA) was performed on a TGA Q50 V6.7 Build 203, Universal V4.5A (TA Instruments, New Castle, DE, USA) equipped with a platinum cell. The scanning range was $30\text{--}600^\circ\text{C}$ using a heating rate of $10^\circ\text{C min}^{-1}$. The temperature for different percentages of weight loss, temperature at maximum decomposition, and residue level at 600°C of NRBC composite films were measured from the TGA curves.

The performance of NRBC composite films such as thermal phase change, glass transition temperature (T_g), crystalline melt temperature (T_m), and thermal stability was measured by differential scanning calorimetry (DSC). Samples about 3–5 mg were sealed in an aluminum pan. The sample was measured under a nitrogen atmosphere. To evaluate the curing behavior, nonisothermal DSC analysis of samples was performed using a NETZSCH DSC 204 F1

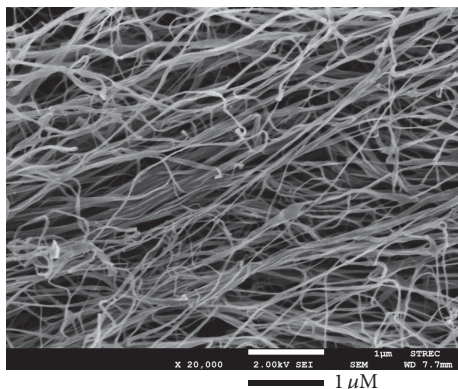


FIGURE 1: SEM image of BC fibers from the dried BC slurry.

Phoenix (Selb, Germany). The samples were heated from -100 to 300°C at a rate of $10^{\circ}\text{C min}^{-1}$.

For tensile property testing, NRBC films were cut into strips 1 cm wide and 10 cm long. The maximum tensile strength and break strain of NRBC composite films were determined with a Lloyd 2000R (Southampton, UK) universal testing machine. The test conditions followed ASTM D882. The tensile strength and break strain were the average values determined from five specimens.

3. Results and Discussion

3.1. Morphology of BC Fiber. The SEM image of the BC slurry is shown in Figure 1. BC was in the form of a small sheet composed of nanofiber networks with an average fiber diameter of approximately $0.05\ \mu\text{m}$, which was about 10% of fiber diameter of regenerated plant cellulose (Whatman filters, catalog no. 1822070 Whatman International Ltd., Maidstone, UK) [21]. Moreover, BC fibers are entirely free of lignin and hemicelluloses. Hence, unlike celluloses of plant origin, the strong treatment of impurity removing was not required for BC preparation [22].

3.2. SEM Analysis of NR, BC, and NRBC Films. Previously, there was a report of reinforced natural rubber with BC nanofibers with BC loading up to 10 wt.% [17]. From our preliminary study, it was found that by adding BC fiber in form of dry/wet fibers or dense slurry, the weight ratio of BC was limited at about 10 wt.% due to poor dispersion of the fibers in NR matrix. In order to improve dispersion of BC nanofibers in the NR latex, BC fibers have to be added in form of dilute slurry of BC in DI water (with the BC concentration of about 1 g of dry weight/100 mL). The mixture of BC and NR should be in form of dilute suspension (not viscous suspension). Well dispersion of BC nanofibers in the NR latex could be obtained by a thorough mixing of dilute BC slurry with natural rubber latex (NRL). By this modification method, higher amount of BC nanofibers (up to weight ratio of 80%) could be added to fabricate the thin films of NRBC composites. SEM was employed to study the outer surface and cross-sectional morphologies of NR, BC, and NRBC films (Figure 2). BC nanofibers in form of swollen fibers in water

(BC slurry) were added and homogeneously mixed with NRL at the weight ratios (based on dry basis) of 20–80 wt.% with good BC fiber dispersion and distribution in NR matrix. NR film had a smooth outer surface compared with those of NRBC and BC films. SEM images of enlarged views of the cross section of the NRBC composite films in Figure 2 show a good dispersion of BC fibers in the NR matrix without extensive aggregation and agglomeration. NRBC20 films had a relatively smooth surface, whereas NRBC40, NRBC60, and NRBC80 films, which contained higher concentrations of BC, showed rough surfaces. According to the cross-sectional views, the nanocellulose fibrils were dispersed consistently within the NR matrix without segregation between fibers and NR. Layered structure or laminated structure were displayed in the BC film and NRBC films with BC loading content at ≥ 40 wt.%. Previously, due to the difference of polarities between NR and cellulose fibers, the development of NR-cellulose composites was limited by nonhomogeneous dispersion of cellulose particles in a rubber matrix. For example, loading of cellulose nanowhiskers (CNWs) at concentrations ≥ 10 wt.% in cross-linked NR nanocomposites by using a two-roll mixing-mill caused aggregation of CNWs in the NR matrix [23]. However, it was shown in this study that the composite films of NR reinforced with BC could be successfully developed by loading BC in form of BC slurry at 20–80 wt.% (dry basis) via a latex aqueous microdispersion process.

3.3. FTIR Analysis. The FTIR spectra (Figure 3) show pure NR absorptions at $2958\ \text{cm}^{-1}$, which are assigned to asymmetric stretching vibration of methyl groups ($-\text{CH}_3$). The peak of symmetric stretching vibration of methylene ($-\text{CH}_2$) at $2918\ \text{cm}^{-1}$ is also presented. The $\text{C}=\text{C}$ stretching is situated at $1652\ \text{cm}^{-1}$. For pure BC, there is a broad peak of $\text{O}-\text{H}$ stretching of hydroxyl group at $3336\ \text{cm}^{-1}$. The absorption band located at $2889\ \text{cm}^{-1}$ is attributed to CH_2 groups [23], and a peak at $1107\ \text{cm}^{-1}$ is attributed to $\text{C}-\text{O}$ symmetric stretching [24]. The FTIR spectra of NRBC composites show peaks around 2949–2955, 2889–2907, and $1652\ \text{cm}^{-1}$, which are assigned to $-\text{CH}_3$, $-\text{CH}_2$, and $\text{C}=\text{C}$ stretching, respectively, and there are peaks of $\text{O}-\text{H}$ stretching at 3340 – $3356\ \text{cm}^{-1}$ and $\text{C}-\text{O}$ stretching at $1107\ \text{cm}^{-1}$. Observations show peaks of NRBC composites consisting of NR and BC. The positions of $-\text{CH}_3$, $-\text{CH}_2$, and $\text{O}-\text{H}$ stretching peaks of NRBC composites were slightly shifted compared with those of the peaks of the reactants, implying some weak interactions without a chemical reaction, which should be interfacial interaction between the filler and NR matrix [10]. For the effects of BC fiber content on the patterns of functional groups in NRBC composites, the peak area of the hydroxyl group was increased with increasing BC fiber content, whereas peak areas of methyl and methylene groups were decreased.

3.4. Degrees of Opacity. Opacity is the degree to which light is not allowed to pass through a material. For packaging applications, the opacity of films is an important factor because it affects the visibility of the packaged product to

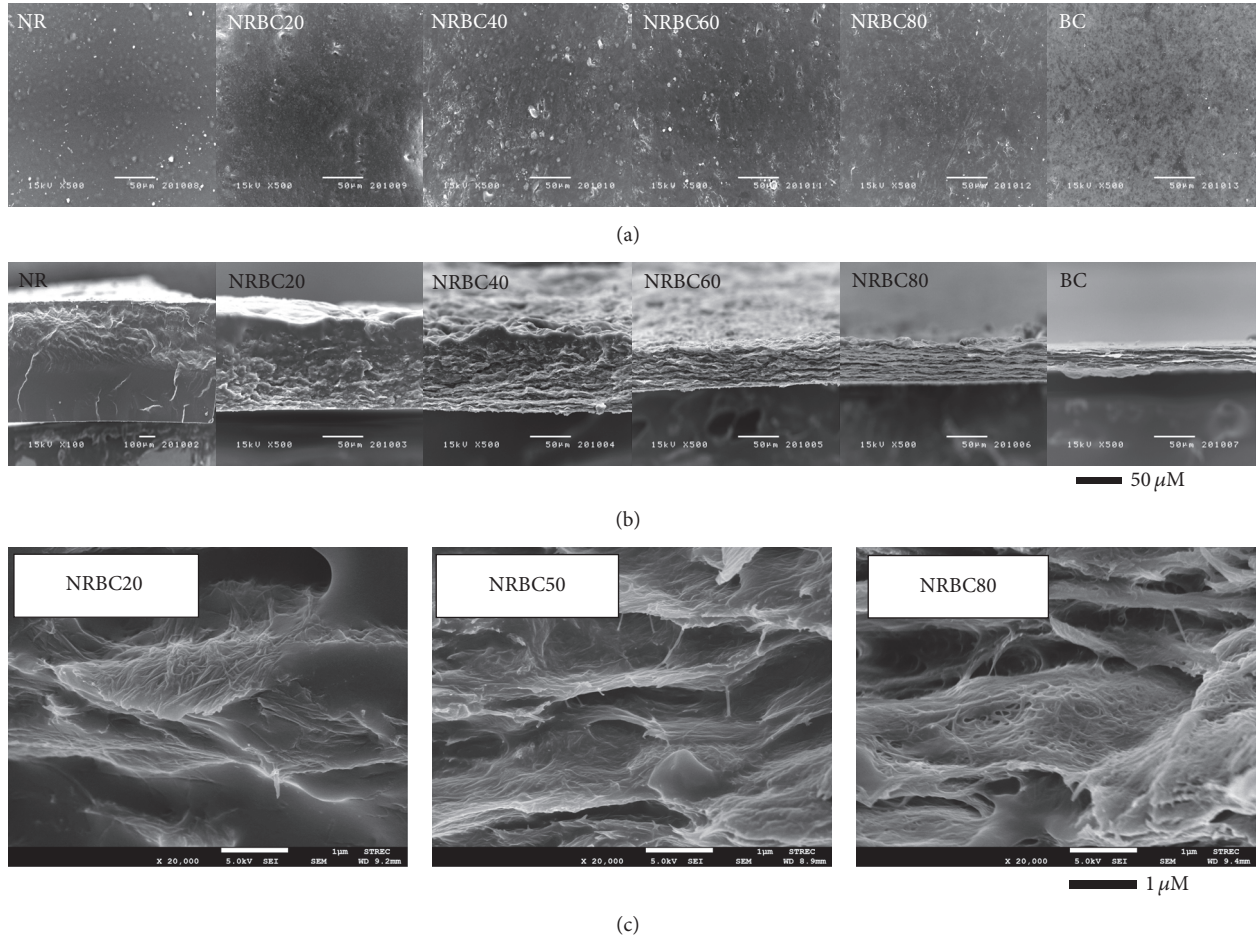


FIGURE 2: SEM images of the films of NR, BC, and NRBC composites: surface views (a), cross section views (b), and enlarged views of the cross section (c).

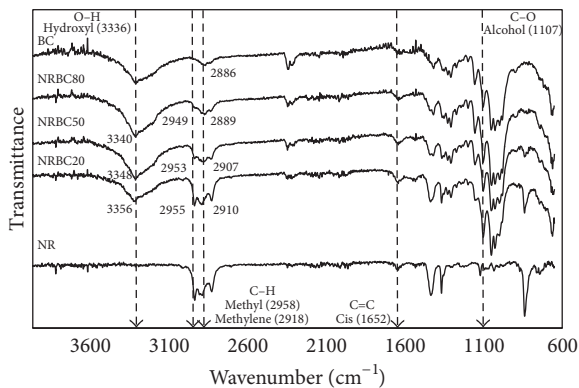


FIGURE 3: FTIR spectra of NR, BC, and NRBC composites.

consumers [25]. The degrees of opacity of NR and BC measured by the UV-Vis Spectrophotometer were 1.31 and 33.10, respectively. The incorporation of BC, which was in the form of a network of nanocellulose fibers in the NR matrix, increased the opacity of films. As shown in Table 1, the degree of opacity of composite films increased proportionally with the increase of BC fiber content in the composite films

because the distribution of cellulose fibers in NR matrix reduced the transparency of the films.

3.5. Contact Angle of Water. The contact angle was used to examine the changes in hydrophilicity of the NRBC composites as shown in Table 1. The particles rich in hydroxyl groups have high hydrophilic characteristics [26]. BC is a hydrophilic substance [27]; the water contact angle of BC was around $47.5^\circ \pm 2.8$. NR is a hydrophobic substance; the water contact angle was around $116.2^\circ \pm 7.8$. The dynamic water contact angle of the NRBC decreased with the increase of BC loading. The polarity, which affects hydrophilicity, was enhanced with the increase of OH groups on the surface of the NRBC composite films. At higher BC loading, the amount of hydroxyl groups increased, resulting in improvement in the hydrophilicities of the films' surfaces (smaller contact angles). Additionally, the surface morphology might also affect contact angle values. The water contact angle was found to be decreased due to an increase in surface roughness [28]. Hydrophilicity of the films will affect absorption capacity and solubility in polar and nonpolar solvents. These properties are important and should be investigated further for the application.

TABLE 1: Degree of opacity and dynamic water contact angles of NR, BC, and NRBC composites.

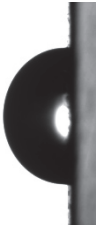
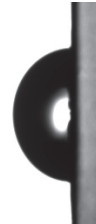
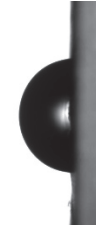
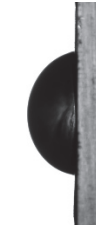

Samples	NR	NRBC20	NRBC50	NRBC80	BC
Opacity ($\times 10^{-3}$)	1.31 ± 0.22 116.21 ± 7.76	6.48 ± 0.12 105.63 ± 2.01	17.70 ± 0.47 90.65 ± 5.12	29.92 ± 0.31 88.32 ± 5.48	33.10 ± 0.28 47.47 ± 2.77
Contact angel ($^{\circ}$)					

TABLE 2: Degree of crystallinity and mechanical properties of NR, BC, and NRBC composites.

Samples	Crystallinity			Mechanical properties		
	Crystalline area	Amorphous area	Degree of crystallinity* (%)	Modulus (MPa)	Tensile (MPa)	Elongation at break (%)
NR	206	18574	1.10	1.6 ± 0.4	0.8 ± 0.1	111.5 ± 6.4
NRBC20	2267	10391	17.91	244.7 ± 53.5	14.6 ± 3.4	14.6 ± 3.1
NRBC50	2571	5197	33.10	2316.0 ± 303.3	45.9 ± 9.6	6.4 ± 3.2
NRBC80	2479	4352	36.29	4128.4 ± 998.3	75.1 ± 27.1	4.3 ± 1.4
BC	4479	3219	58.18	2288.8 ± 1585.5	54.0 ± 7.6	5.5 ± 2.7

*Degree of crystallinity = crystalline area/total area.

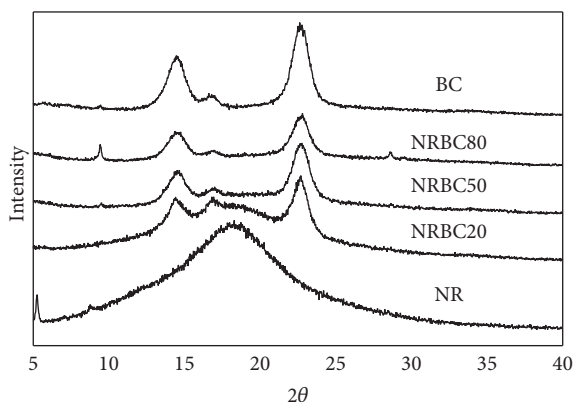


FIGURE 4: XRD patterns of NR, BC, and NRBC composites.

3.6. Crystallinity. The XRD patterns of NR, BC, and NRBC composite films are shown in Figure 4. The XRD pattern of BC showed peaks at 14.1°, 16.1°, and 22.4° [29–31]. The XRD pattern of amorphous NR did not show any sharp peaks. The XRD patterns of NRBC composite films also showed three peaks, and their locations were similar to those of BC. Compared with the other patterns, the diffraction peaks of BC were sharp and highly dense. The crystallinity of the NRBC composite films increased with an increase in the amount of BC incorporated into the NR matrix (Table 2). It was suggested that the filler exists in crystalline phase in the matrix. The incorporation of high crystalline fibers in amorphous region of NR polymer could create strains encouraged localized crystallinity [32].

3.7. Thermal Degradation. The thermal degradations of the NR, NRBC, and BC films were presented in terms of percentage weight loss versus temperature (Figure 5). The degradation of polymers indicates chain scission, cross-link formation, and cross-link breakage [33]. When the films were heated at a temperature below 200°C, volatile components, such as moisture or solvent, evaporated. On heating above 200°C, polymer degradation into gaseous products was observed. Then, the heating removes all organic matter, leaving a residue of inorganic fillers in the composites [23]. The peak at 59°C of BC was for the evaporation of water, which was 15% of the initial weight. The polymer decomposition temperatures were 230–300°C and 230–490°C for BC and NR

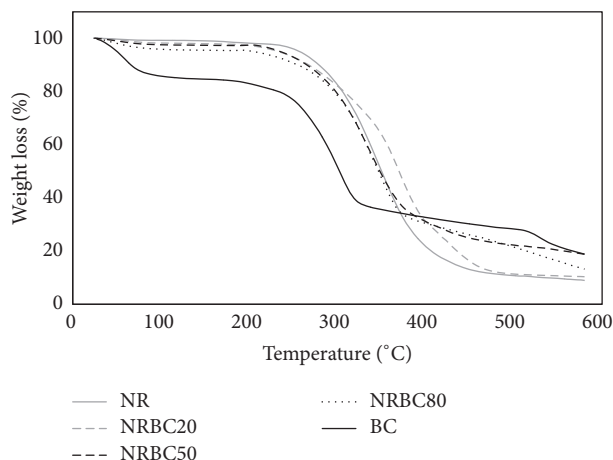


FIGURE 5: Weight loss of NR, BC, and NRBC composites.

films, respectively. The NRBC composites showed peaks of the polymer decomposition after water evaporation, similar to those of NR. The results from the TGA curves indicate that the NRBC composites could be used for applications at temperature up to approximately 230°C. It was noticed that the decomposition of NRBC20 slightly shifted to higher temperature as compared with those of pure NR and the other NRBC composites, which could indicate a higher thermal stability of NRBC20. It has been previously shown that NRBC20 was more homogeneous with a denser structure (Figure 2). In addition, a higher shift in position of O–H stretching of hydroxyl group, which reflected more interaction between NR and BC, was also observed in NRBC20 as compared to those of the other NRBC composites (Figure 3). With good distribution and dispersion of nanofibers in NR matrix, the interfacial adhesion between fibers and NR matrix could be enhanced, resulting in more interaction between NR and BC. Oppositely, agglomeration of fillers or poor distribution of fibers in the matrix could worsen the interfacial adhesion and bonding of the composites [10]. The further heating removed all organic matter, yielding the weight of residual char. The char yields of NR and NRBC20 were lower than those of NRBC50, NRBC80, and BC. When heated up to 580°C, the char yields of NR, NRBC20, NRBC50, NRBC80, and BC were 8.96%, 10.33%, 13.22%, 18.83%, and 18.86%, respectively. Similar TGA patterns of NR, cellulose, and their

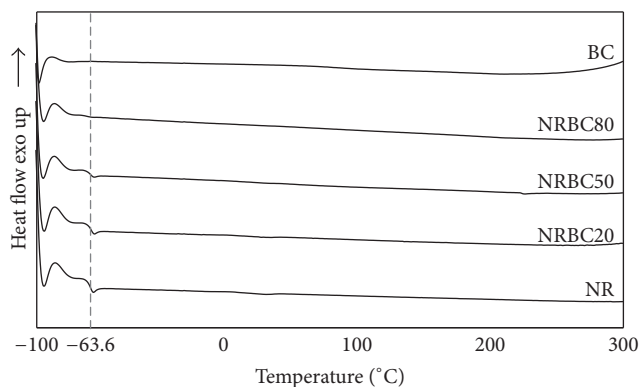


FIGURE 6: DSC chromatograms of NR, BC, and NRBC composites.

composites were previously reported in the study of NR reinforced with nanocelluloses isolated from raw jute fibers by a steam explosion process [23, 33].

3.8. DSC Chromatograms. The DSC chromatograms of NR, BC, and NRBC composites performed at -100 to 300°C were shown in Figure 6. Pure NR chromatograms showed T_g at -63.6°C , whereas pure BC remained unchanged in the range from -100 to 300°C . The composite chromatograms showed T_g values at -63.4 , -63.8 , and -66.5°C for NRBC20, NRBC50, and NRBC80, respectively. Generally, the crystalline portion remains crystalline during the glass transition, whereas at a low temperature the amorphous regions of a polymer become in the glassy state. According to the observation from SEM images (Figure 2), the formation of the NRBC composites with a weight ratio of BC $\geq 50\%$ exhibited multilayered porous structures. The reinforcement by adding BC fibers with a high weight ratio of BC (NRBC50, NRBC80) caused a slightly lower T_g . A low T_g indicates higher polymer flexibility or mobility [34, 35]. A polymer chain should be more flexible and could move easier in a multilayered porous structure and the microstructure of a polymer has an important impact on T_g . Therefore, the multilayered porous structure of NRBC 50 and NRBC 80 might lead to the slightly decreased T_g of these composites.

3.9. Mechanical Properties. Young's modulus, tensile strength, and elongation at break determined from the stress-strain curves are shown in Figure 7. Elastic elongation is the most important characteristic of NR. Pure NR film has a high elastic elongation but low tensile strength. The elongation of NR is very well known at around 700–1000%. The elongation at break of the NR thin film fabricated in the present work was quite low ($111.5 \pm 6.4\%$). The alteration of a mechanical property should be due to the differences in materials and procedures for the film formation. In Thailand, the natural rubber latex was normally preserved by addition of preservative agents such as ammonia, tetramethylthiuram disulfide (TMTD), and zinc oxide in order to prevent coagulation. The types and concentrations of preservative agents might also have an effect on the property of NR film.

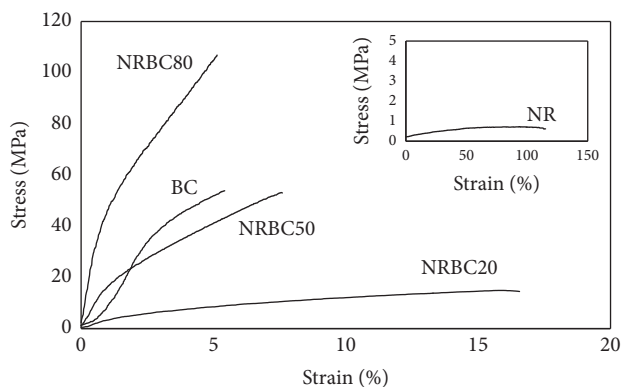


FIGURE 7: Stress-strain curve of NR, BC, and NRBC composites.

The stress-strain profiles of the NRBC composites (Figure 7) show considerably higher modulus and tensile strength than those of NR. The modulus was increasingly enhanced with the increase of BC fiber content because of the inclusion of crystalline BC fiber into the rubber matrix. When crystalline cellulose was added to the amorphous matrix of NR, the crystallinity of the composite probably dominates the bulk properties, increasing modulus values [36–38]. NR film is soft and tough. NRBC20 preserved the elastic features of NR with lower elongation than NR due to the presence of BC nanofibers in NR matrix. NRBC80 showed considerable improvement in mechanical properties such as Young's modulus and tensile strength, influenced by the presence of BC nanofibers at high content. Because of the high crystallinity of BC, NRBC80 is hard and strong. The mechanical properties NRBC50 were between those of NRBC20 and NRBC80.

Young's modulus, tensile strength, and elongation at break of dry films of NR, BC, and NRBC composites at different BC loading contents are shown in Table 2. Pure NR film showed a low Young's modulus and low tensile strength but high elongation at break. Conversely, BC showed a high Young's modulus and high tensile strength but low elongation at break. Young's moduli and tensile strengths of the NRBC films were enhanced as the BC fiber content was increased. NRBC80 had the highest Young's modulus and tensile strength at 4,128.4 and 75.1 MPa, respectively, which were also significantly higher than those of the BC film. It was suggested that NR chains might be immobilized by the network of nanocellulose fibers led to significant enhancement of mechanical strength of the NRBC composite [17, 38]. Young's modulus and tensile strength of NRBC80 are considered very high as compared to other NR composites. According to the report of regenerated cellulose-epoxidized natural rubber (RC/ENR) blended films with the 80 wt.% of RC, Young's modulus and tensile strength were 2490 and 45.1 MPa, respectively [39]. The modulus of NRBC80 was ≥ 400 times those of NR composites reinforced with cellulosic materials from plants [23, 40, 41]. However, there are limitations of reinforcement such as decreases in elasticity. Decreased elongations at break of the composites were observed as the BC loading content was increased. Moreover, the compatibility and homogeneity of NR and BC in the

composites were relatively reduced at higher BC loading content. The composite of NRBC20 showed an average elongation at break at 14.6%, which was about 13.1% of that of pure NR. Reinforcement with the smaller particles has shown better mechanical properties than reinforcement with large particles in filled NR [6]. Due to the excellent mechanical properties of BC nanofibers, the reinforcement of NR with BC via a latex aqueous microdispersion process considerably enhanced Young's modulus and tensile strength of the NRBC composites, which are considered very high compared with the composites of NR reinforced with cellulose nanowhiskers isolated from bamboo waste [23] and nanocellulose isolated from raw jute fiber [41].

4. Conclusion

NRBC composite films were successfully prepared via a latex aqueous microdispersion process. BC nanofibers in slurry form at loading contents from 20 to 80 wt.% (dry basis) were well dispersed and well distributed within the NR matrix. Interfacial interactions between BC fibrils and NR were illustrated by FTIR and DSC analysis. The hydrophilicity, opacity, and crystallinity of the NRBC composite films increased with the increase of BC loading content. The mechanical properties were effectively enhanced via reinforcement by BC nanofibers. NRBC80, which was a hard and strong biocomposite film, had the highest Young's modulus at 4,128.4 MPa and tensile strength of 75.1 MPa. On the other hand, NRBC20 exhibited high elastic elongation at 14.6% with relative improvements in Young's modulus, tensile strength, and thermal stability in comparison with those of pure NR. The mechanical strength of the NRBC composite films was considered high compared with those of the composites of NR reinforced with other nanocelluloses. Because of its excellent mechanical properties and thermal stability, the NRBC composites are expected to have high potential uses as rubber-based products or elastic packaging in many applications, including food and medical applications.

Competing Interests

The authors declare that there is no conflict of interests regarding the publication of this paper.

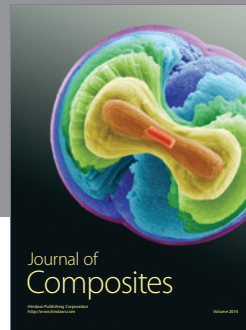
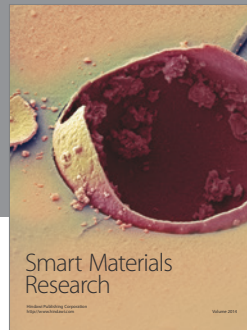
Acknowledgments

This work was supported by the Ratchadaphiseksomphot Endowment Funds, Chulalongkorn University, Project CU-58-032-AM, and the Institutional Research Grant (the Thailand Research Fund), IRG 5780014, and Chulalongkorn University, Contract no. RES_57_411_21_076.

References

- [1] A. D. Roberts, *Natural Rubber Science and Technology*, Oxford University Press, 1988.
- [2] A. Thorn and R. Robinson, "Compound design," in *Rubber Products Manufacturing Technology*, Marcel Dekker Inc, New York, NY, USA, 1994.
- [3] J. L. Leblanc, "Rubber-filler interactions and rheological properties in filled compounds," *Progress in Polymer Science*, vol. 27, no. 4, pp. 627–687, 2002.
- [4] Z. X. Ooi, H. Ismail, and A. A. Bakar, "Optimisation of oil palm ash as reinforcement in natural rubber vulcanisation: a comparison between silica and carbon black fillers," *Polymer Testing*, vol. 32, no. 4, pp. 625–630, 2013.
- [5] Y. Ikeda and S. Kohjiya, "In situ formed silica particles in rubber vulcanizate by the sol-gel method," *Polymer*, vol. 38, no. 17, pp. 4417–4423, 1997.
- [6] V. Tangpasuthadol, A. Intasiri, D. Nuntivanich, N. Niyompanich, and S. Kiatkamjornwong, "Silica-reinforced natural rubber prepared by the sol-gel process of ethoxysilanes in rubber latex," *Journal of Applied Polymer Science*, vol. 109, no. 1, pp. 424–433, 2008.
- [7] N. Watcharakul, S. Poompradub, and P. Prasassarakich, "In situ silica reinforcement of methyl methacrylate grafted natural rubber by sol-gel process," *Journal of Sol-Gel Science and Technology*, vol. 58, no. 2, pp. 407–418, 2011.
- [8] Q. Wang, Y. Luo, C. Feng et al., "Reinforcement of natural rubber with core-shell structure silica-poly(methyl methacrylate) nanoparticles," *Journal of Nanomaterials*, vol. 2012, Article ID 782986, 5 pages, 2012.
- [9] N. Y. Yuhana, S. Ahmad, M. R. Kamal, S. C. Jana, and A. R. S. Bahri, "Morphological study on room-temperature-cured PMMA-grafted natural rubber-toughened epoxy/layered silicate nanocomposite," *Journal of Nanomaterials*, vol. 2012, Article ID 760401, 14 pages, 2012.
- [10] Y. Zhou, M. Fan, L. Chen, and J. Zhuang, "Lignocellulosic fibre mediated rubber composites: an overview," *Composites Part B: Engineering*, vol. 76, pp. 180–191, 2015.
- [11] J. Wang and D. Chen, "Mechanical properties of natural rubber nanocomposites filled with thermally treated attapulgite," *Journal of Nanomaterials*, vol. 2013, Article ID 496584, 11 pages, 2013.
- [12] D. Klemm, D. Schumann, U. Udhardt, and S. Marsch, "Bacterial synthesized cellulose—artificial blood vessels for microsurgery," *Progress in Polymer Science*, vol. 26, no. 9, pp. 1561–1603, 2001.
- [13] D. Klemm, B. Heublein, H.-P. Fink, and A. Bohn, "Cellulose: fascinating biopolymer and sustainable raw material," *Angewandte Chemie—International Edition*, vol. 44, no. 22, pp. 3358–3393, 2005.
- [14] W. K. Czaja, D. J. Young, M. Kawecki, and R. M. Brown Jr., "The future prospects of microbial cellulose in biomedical applications," *Biomacromolecules*, vol. 8, no. 1, pp. 1–12, 2007.
- [15] E. Trovatti, L. Oliveira, C. S. R. Freire et al., "Novel bacterial cellulose-acrylic resin nanocomposites," *Composites Science and Technology*, vol. 70, no. 7, pp. 1148–1153, 2010.
- [16] E. Trovatti, S. C. M. Fernandes, L. Rubat et al., "Pullulan-nanofibrillated cellulose composite films with improved thermal and mechanical properties," *Composites Science and Technology*, vol. 72, no. 13, pp. 1556–1561, 2012.
- [17] E. Trovatti, A. J. F. Carvalho, S. J. L. Ribeiro, and A. Gandini, "Simple green approach to reinforce natural rubber with bacterial cellulose nanofibers," *Biomacromolecules*, vol. 14, no. 8, pp. 2667–2674, 2013.
- [18] T. Manzur, N. Yazdani, and Md. A. B. Emon, "Effect of carbon nanotube size on compressive strengths of nanotube reinforced cementitious composites," *Journal of Materials*, vol. 2014, Article ID 960984, 8 pages, 2014.
- [19] M. A. López-Mata, S. Ruiz-Cruz, N. P. Silva-Beltrán, J. D. J. Ornelas-Paz, P. B. Zamudio-Flores, and S. E. Burrueal-Ibarra,

- “Physicochemical, antimicrobial and antioxidant properties of chitosan films incorporated with carvacrol,” *Molecules*, vol. 18, no. 11, pp. 13735–13753, 2013.
- [20] A. Jokar, M. H. Azizi, and Z. Hamidi Esfehiani, “Effects of ultrasound time on the properties of polyvinyl alcohol-based nanocomposite films,” *Nutrition and Food Sciences Research*, vol. 2, no. 4, pp. 29–38, 2015.
- [21] M. Phisalaphong, T. Suwanmajo, and P. Sangtherapitikul, “Novel nanoporous membranes from regenerated bacterial cellulose,” *Journal of Applied Polymer Science*, vol. 107, no. 1, pp. 292–299, 2008.
- [22] W. Czaja, A. Krystynowicz, S. Bielecki, and R. M. Brown, “Microbial cellulose—the natural power to heal wounds,” *Bio-materials*, vol. 27, no. 2, pp. 145–151, 2006.
- [23] P. M. Visakh, S. Thomas, K. Oksman, and A. P. Mathew, “Crosslinked natural rubber nanocomposites reinforced with cellulose whiskers isolated from bamboo waste: processing and mechanical/thermal properties,” *Composites Part A: Applied Science and Manufacturing*, vol. 43, no. 4, pp. 735–741, 2012.
- [24] A. Stoica-Guzun, M. Stroescu, S. I. Jinga et al., “Box-Behnken experimental design for chromium(VI) ions removal by bacterial cellulose-magnetite composites,” *International Journal of Biological Macromolecules*, vol. 91, pp. 1062–1072, 2016.
- [25] C. K. Saurabh, S. Gupta, J. Bahadur, S. Mazumder, P. S. Variyar, and A. Sharma, “Mechanical and barrier properties of guar gum based nano-composite films,” *Carbohydrate Polymers*, vol. 124, pp. 77–84, 2015.
- [26] Y. Ye, C. Zhang, M. Tian, Z. Du, and J. Mi, “Macroscopic and microscopic analyses of hydrophobic modification of rubbers with silica nanoparticles,” *Journal of Physical Chemistry C*, vol. 119, no. 36, pp. 20957–20966, 2015.
- [27] Y. Yuan and T. R. Lee, “Contact angle and wetting properties,” in *Surface Science Techniques*, vol. 51 of *Springer Series in Surface Sciences*, pp. 3–34, Springer, Berlin, Germany, 2013.
- [28] S. Kirdponpattara, B.-M. Z. Newby, and M. K. Phisalaphong, “Effect of oxygen plasma treatment on bacterial cellulose-alginate composite sponge as a yeast cell carrier for ethanol fermentation,” in *Advanced Materials Research*, pp. 1150–1153, Trans Tech Publications, Zurich, Switzerland, 2013.
- [29] L. Hong, Y. L. Wang, S. R. Jia, Y. Huang, C. Gao, and Y. Z. Wan, “Hydroxyapatite/bacterial cellulose composites synthesized via a biomimetic route,” *Materials Letters*, vol. 60, no. 13–14, pp. 1710–1713, 2006.
- [30] S. Keshk and K. Sameshima, “Influence of lignosulfonate on crystal structure and productivity of bacterial cellulose in a static culture,” *Enzyme and Microbial Technology*, vol. 40, no. 1, pp. 4–8, 2006.
- [31] M. Phisalaphong and N. Jatupaiboon, “Biosynthesis and characterization of bacteria cellulose–chitosan film,” *Carbohydrate Polymers*, vol. 74, no. 3, pp. 482–488, 2008.
- [32] A. Sonia and K. Priya Dasan, “Celluloses microfibers (CMF)/poly (ethylene-co-vinyl acetate) (EVA) composites for food packaging applications: a study based on barrier and biodegradation behavior,” *Journal of Food Engineering*, vol. 118, no. 1, pp. 78–89, 2013.
- [33] E. Abraham, M. S. Thomas, C. John, L. A. Pothen, O. Shoseyov, and S. Thomas, “Green nanocomposites of natural rubber/nanocellulose: membrane transport, rheological and thermal degradation characterisations,” *Industrial Crops and Products*, vol. 51, pp. 415–424, 2013.
- [34] W. Pichayakorn, J. Suksaeree, P. Boonme, W. Taweepreda, and G. C. Ritthidej, “Preparation of deproteinized natural rubber latex and properties of films formed by itself and several adhesive polymer blends,” *Industrial & Engineering Chemistry Research*, vol. 51, no. 41, pp. 13393–13404, 2012.
- [35] S. Honary and H. Orafi, “The effect of different plasticizer molecular weights and concentrations on mechanical and thermomechanical properties of free films,” *Drug Development and Industrial Pharmacy*, vol. 28, no. 6, pp. 711–715, 2002.
- [36] H. Ismail, M. R. Edyham, and B. Wirjosentono, “Bamboo fibre filled natural rubber composites: the effects of filler loading and bonding agent,” *Polymer Testing*, vol. 21, no. 2, pp. 139–144, 2002.
- [37] A. Karmarkar, S. S. Chauhan, J. M. Modak, and M. Chanda, “Mechanical properties of wood-fiber reinforced polypropylene composites: effect of a novel compatibilizer with isocyanate functional group,” *Composites Part A: Applied Science and Manufacturing*, vol. 38, no. 2, pp. 227–233, 2007.
- [38] M. G. Thomas, E. Abraham, P. Jyotishkumar, H. J. Maria, L. A. Pothen, and S. Thomas, “Nanocelluloses from jute fibers and their nanocomposites with natural rubber: preparation and characterization,” *International Journal of Biological Macromolecules*, vol. 81, pp. 768–777, 2015.
- [39] M. Soheilmoghaddam, M. U. Wahit, and N. Ibrahim Akos, “Regenerated cellulose/epoxidized natural rubber blend film,” *Materials Letters*, vol. 111, pp. 221–224, 2013.
- [40] J. Bras, M. L. Hassan, C. Bruzesse, E. A. Hassan, N. A. El-Wakil, and A. Dufresne, “Mechanical, barrier, and biodegradability properties of bagasse cellulose whiskers reinforced natural rubber nanocomposites,” *Industrial Crops and Products*, vol. 32, no. 3, pp. 627–633, 2010.
- [41] E. Abraham, P. A. Elbi, B. Deepa et al., “X-ray diffraction and biodegradation analysis of green composites of natural rubber/nanocellulose,” *Polymer Degradation and Stability*, vol. 97, no. 11, pp. 2378–2387, 2012.



Hindawi

Submit your manuscripts at
<https://www.hindawi.com>

